JOURNAL OF PROPULSION AND POWER
Vol. 12, No. 5, September–October 1996

Early Results from Solar Dynamic Space Power System Testing

Richard K. Shaltens* and Lee S. Mason†
NASA Lewis Research Center, Cleveland, Ohio 44135

A government/industry team designed, built, and tested a 2-kWe solar dynamic space power system in a large thermal/vacuum facility with a simulated sun at the NASA Lewis Research Center. The Lewis facility provides an accurate simulation of temperatures, high vacuum, and solar flux as encountered in low-Earth orbit. The solar dynamic system includes a Brayton power conversion unit integrated with a solar receiver that is designed to store energy for continuous power operation during the eclipse phase of the orbit. This article reviews the goals and status of the Solar Dynamic Ground Test Demonstration project and describes the initial testing, including both operational and performance data. System testing to date has accumulated over 365 h of power operation (ranging from 400 W to 2.0 kWe), including 187 simulated orbits, 16 ambient starts, and two hot restarts. Data are shown for an orbital startup, transient and steady-state orbital operation, and shutdown. System testing with varying insolation levels and operating speeds is discussed. The solar dynamic ground test demonstration is providing the experience and confidence toward a successful flight demonstration of the solar dynamic technologies on the Space Station Mir in 1997.

Introduction

THE NASA Office of Space Access and Technology initiated the 2-kWe Solar Dynamic (SD) Ground Test Demonstration (GTD) project.[1,2] The primary goal of this project was to conduct testing of flight prototypical components as part of a complete SD system. Demonstrations of both system power delivered and total system efficiency in low-Earth orbit (LEO) were key test objectives. The SD space power system shown in Fig. 1 includes the solar concentrator and solar receiver with thermal energy storage integrated with the power conversion unit (PCU), installed in a facility simulating an environment representative of LEO.

Programs during the past 30 years have developed SD component technologies that are now available for near-Earth orbit applications. However, several technical challenges identified during the Space Station *Freedom* program are currently being investigated during the GTD testing.[3] These key issues are as follows:

1) Flux tailoring: integration of the concentrator and receiver such that adequate solar flux is transferred into the cycle without excessive flux deposition on any one area of the receiver.

2) Control methodology: investigate methods of varying turboalternator compressor (TAC) speed and system thermal management to maintain optimum system operation (energy management) caused by large time period changes in insolation.

3) Transient-mode performance: evaluation of startup and shutdown transients, and multiple orbit operations.

The SD GTD project has demonstrated a complete SD system in a thermal/vacuum environment, i.e., the large space environmental facility, known as Tank 6, at NASA Lewis Research Center (LeRC). The Tank 6 facility includes a solar simulator to supply the equivalent of one sun, a liquid-nitrogen-cooled wall operating at 78 K (140.4°R), which provides a heat sink to simulate the deep space environment [about 200 K (360°R)], and an electric load simulator capable of dissipating up to 4 kW of electrical power. Testing in December 1994 resulted in the world's first operation of a complete SD system in a relevant environment. SD system testing has demonstrated orbital startup, transient and steady-state orbital operation, and shutdown. Flight typical components were used in the SD system wherever possible to demonstrate the availability of SD technologies. Only the power conditioning, control system, and parasitic load radiator were not flight hardware designs. An overview of the GTD activities is provided by Shaltens and Boyle.[4–6]

Solar Simulator

The LeRC solar simulator design consists of nine 30-kW xenon arc lamps and provides a nominal flux of 1.37 kW/m^2 with a subtense angle of about 1.0 deg for testing solar dynamic systems. A photograph of the advanced solar simulator (in the upper left) next to the vacuum tank is shown in Fig. 2.

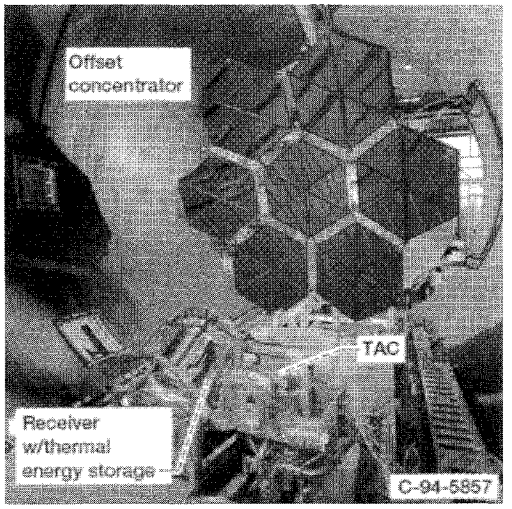

Fig. 1 Photograph of the solar dynamic system.

Received Oct. 6, 1995; revision received April 15, 1996; accepted for publication April 30, 1996.

*Manager, Solar Dynamic Ground Test Demonstration Project.

†Test Director, Solar Dynamic Ground Test Demonstration Project.

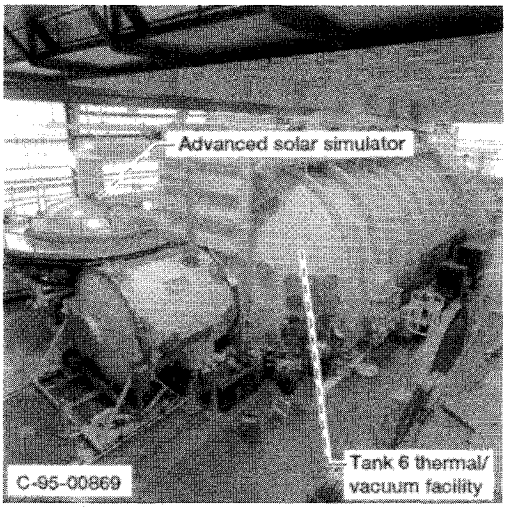

Fig. 2 Photograph of the solar simulator and Tank 6.

This solar simulator provides an apparent sun just outside the vacuum tank that shines through a quartz window into the tank to provide the desired flux (up to 1.66 kW/m^2) at the target area. The target area (i.e., concentrator interface) is 4.79 m in diameter and 17.2 m from the apparent sun. A water-cooled shutter is opened and closed to simulate various orbits. The advanced solar simulator system design results in a 50% improvement in the solar simulator system efficiency when compared to conventional designs. An advanced optics system design (new collector and lens), results in the use of only nine 30-kW arc lamps rather than 19 arc lamps with a conventional optics system.[7] This significantly reduces its size and initial cost as well as future operating and maintenance costs. Fabrication, assembly, installation, and checkout of the solar simulator integrated with Tank 6 were completed in September 1994. A detailed description of the solar simulator design and results from early testing of a subscale optics system are discussed by Jefferies,[7] while the initial operation is discussed by Jaworske.[8]

Solar Dynamic System

The SD system includes the following major subsystems: 1) a solar concentrator, 2) a solar receiver with thermal energy storage, 3) a power-conversion system, 4) a waste heat rejection (WHR) system, and 5) a power conditioning and control system. The SD system was designed to produce about 2 kWe (at 120 Vdc) utilizing thermal energy storage with an overall system efficiency greater than 15%. It should be noted that the system performance and life were not optimized because of the constraints of utilizing existing hardware designed for other applications.

A block diagram of the SD system is shown in Fig. 3. Energy for operating the SD system is obtained by intercepting solar radiation by use of a parabolic solar concentrator. The concentrator focuses the solar radiation into the cavity of the heat receiver. The heat receiver, which incorporates thermal energy storage, serves a dual purpose. During the on-sun phase of the orbit, the receiver transfers the energy to the cycle working fluid and to the phase-change energy storage material. During the eclipse portion of the orbit, the receiver gives up energy from the phase-change material to the cycle working fluid. The hot cycle working fluid exiting the receiver is then expanded through a turbine thereby producing the work necessary to turn the compressor and alternator. The working fluid passes through the recuperator (counterflow heat exchanger), which serves to preheat the fluid entering the receiver, thus increasing cycle efficiency. From the recuperator, the working fluid is then cooled to the compressor inlet temperature by removing the remaining waste heat energy via a gas-to-liquid heat exchanger (gas cooler). The waste heat from the cooler is dissipated by the heat rejection system. The fluid entering the compressor is compressed and used to cool the alternator before it is preheated at the recuperator and passed to the heat receiver.

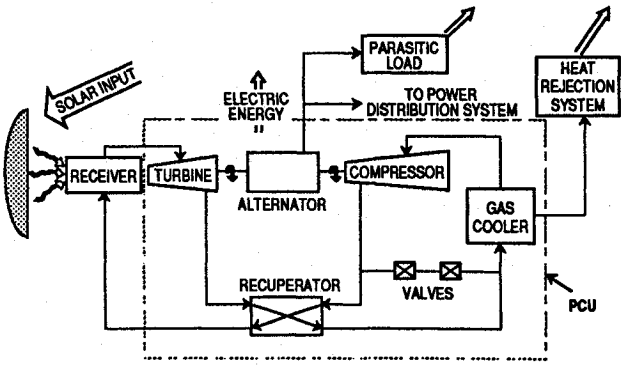

Fig. 3 Block diagram of the solar dynamic system.

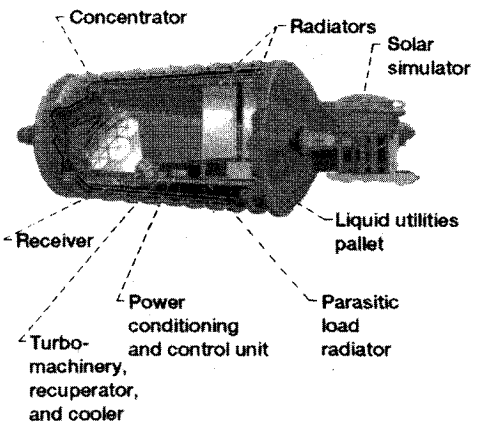

Fig. 4 Solar dynamic system layout in Tank 6.

Design life of the GTD system is for over 1000 h of operation with up to 100 starts from a cold condition. The nominal design case for the GTD was the maximum insolation orbit with 66 min of sun and 27 min of shade.

System Integration

Major components of the GTD system were derived from existing designs. The TAC and recuperator came from the Brayton Isotope Power System[9] and the off-axis concentrator, solar receiver, and radiator were based on designs scaled from Space Station *Freedom*.[2] Components were integrated based on the requirement that their interfaces be as simple as possible and that their function be readily assignable to one or another of the performing organizations. Flight packaging was not pursued because of the desire for modularity of components and simplification of their structural interfaces. The modular design of the SD system also offers the potential to evaluate advanced subsystems and components in the Tank 6 environment at a later date. Figure 4 illustrates the modular layout of the SD components as it is configured in Tank 6.

Concentrator Subsystem

As shown in Fig. 1, the completed offset concentrator structure consists of seven hexagonal panels with six reflective facets (mirrors) per panel.[10] The concentrator is 4.75 m wide by 4.55 m tall and is supported on a leaning tripod support structure that attaches to a removable test stand. Facet reflectivity exceeds 85% and the mass is about 2.5 kg/m^2. After assembly, the concentrator was proof-checked on the test stand followed by facet installation and alignment. A detailed description of the offset concentrator design is provided by Bahnman.[11]

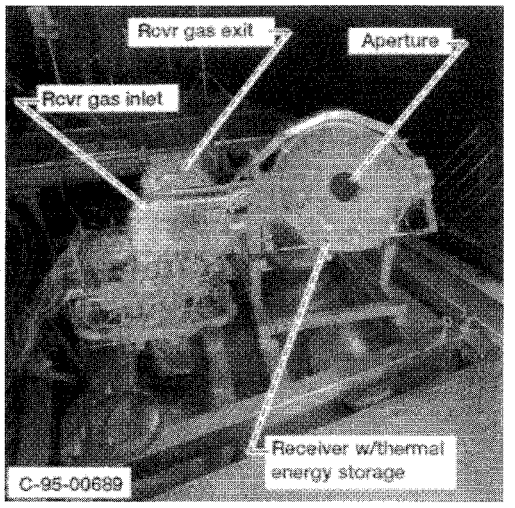

Fig. 5 Completed receiver integrated with the PCU.

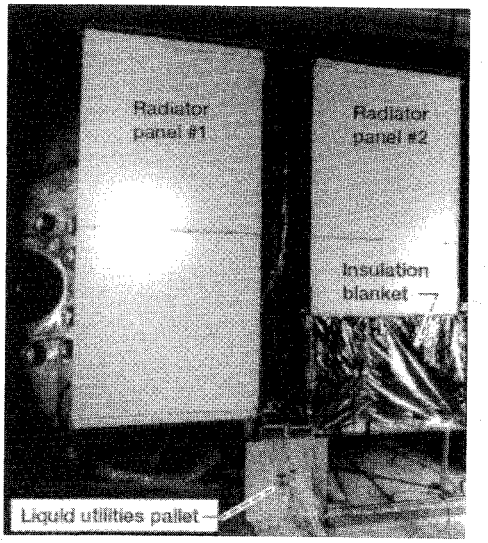

Fig. 6 Completed WHR system.

Receiver and PCU Subsystems

Integration of the completed solar receiver with the PCU is shown in Fig. 5. The receiver is used to transfer the solar thermal energy to the cycle working fluid and to store solar energy for system operation during eclipse. The receiver design is essentially a scale model from the Space Station *Freedom* and uses the same thermal energy storage canister (full size) as was designed, built, and tested during the Space Station *Freedom* program. Manufacturing, development, and testing of the canisters have been completed and are discussed by Strump.[12] The storage canister consists of the Haynes 188 shell, or hollow doughnut, filled with $LiF-CaF_2$ eutectic phase-change material. The phase-change material has a melting point of 1041 K (1873°R). Key additions to the canister tube design that provide enhanced performance are heat transfer fins added to the internal flow path and an alumina-based canister coating[13] for improved thermal emissivity. A complete description of the receiver design is provided by Strumph.[14,15]

The PCU subsystem is a closed Brayton cycle that includes the TAC, gas coolers, recuperator, ducting, and support structure. The TAC, known as the mini-BRU (Brayton rotating unit), consists of a single-stage radial flow compressor, turbine, and a brushless four-pole Rice alternator mounted on a single shaft. Foil gas bearings are used to provide long-life operation by eliminating metal-to-metal contact of the shaft and bearings during operation. The alternator, bearings, and shaft are cooled by the compressor discharge flow. While operating at 54,000 rpm, the TAC can produce electric power up to a maximum of 2.2 kW (at 120 Vdc). The PCU subsystem unit uses a helium–xenon gas mixture with a molecular weight of 83.8 as the working fluid. The gas mixture was optimized for heat transfer and aerodynamic performance for the mini-BRU.[9] The compressed working fluid is preheated in a recuperator by turbine exhaust gases to increase efficiency of the cycle. A detailed discussion of the TAC design is provided by Amundsen.[9] Acceptance testing of the PCU (known as the hot loop test) was completed with the demonstration of 2 kW of electrical power. Testing was performed at local atmospheric conditions with an electrical heater. Prior to integration of the receiver and PCU, each assembly was covered with multilayer foil insulation by wrapping multiple layers of nickel and aluminum foils around the critical hot parts.

WHR Subsystem

Shown in Fig. 6 is the completed WHR system, which consists of two identical radiator panels plumbed in series and a liquid utilities pallet (LUP) in a closed-pumped liquid-loop design. The LUP contains the pump(s), accumulator, sensors, and an auxiliary heater for the *n*-heptane coolant fluid.[16] Each bonded aluminum honeycomb radiator panel is about 1.77 by 3.66 m with a radiating area of 12.96 m^2. Each panel has 11 active and 11 inactive flow tubes evenly spaced to simulate thermal transient response of a fully redundant flow path design. Each panel is coated with a white epoxy paint, chemglaze A276™, a thermal control coating. The WHR system is integrated into the PCU loop by means of two gas-to-liquid heat exchangers, or gas coolers. A detailed description of the analysis, design, fabrication, and testing of the waste heat subsystem is provided by Fleming.[17,18]

Acceptance testing of the waste heat subsystem was completed in the LeRC thermal/vacuum facilities. Both steady-state and transient operation of the WHR system were conducted. Heat rejection during steady-state tests ranged from 2.5 to 6.3 kWt. To meet the desired fluid outlet temperature at GTD nominal operating conditions at the lower, apparent sink temperature, radiator no. 2 was covered with about 1.2 m of insulation blankets. Performance of the WHR system was as expected.

Power Conditioning and Control Subsystem

The power conditioning and control unit (PCCU) contains the power electronics. The start inverter power supply is a commercially available, variable, controllable three-phase power supply that provides the ability to operate the TAC alternator as both an inductive and synchronous electric motor. Starting profiles are being investigated to ascertain, by test, the optimum starting electrical characteristics. The parasitic load radiator is an integral part of the electric loop controls and functions as an electrical sink for excess power (up to 100%) from the TAC that is not consumed by the user load, accessory loads, and PCCU. The parasitic load radiator, which is controlled by the PCCU, consists of an array of vacuum-compatible, individually controlled cal rod heaters with enhanced emissivity characteristics.[13]

The data acquisition and control system (DACS) is special test equipment whose primary function is to record system test data. The DACS also contains the ability to communicate setpoint conditions to the PCCU to vary speed, voltage, and gain setpoints. This allows for changing the control parameters during the system test without the need to physically access the PCCU within the thermal/vacuum environment.

System Operation and Testing

Integrated system testing is being conducted over the system operating range to evaluate and validate previously developed analytical models. Testing was conducted in two phases: 1) system acceptance tests by AlliedSignal, and 2) system characterization tests by NASA.[19] Operation is being conducted to

characterize the SD system and evaluate various analytical models over a variety of solar insolation levels, speed conditions, orbit periods, engine inventories, and radiator variations. Further, development, verification, and qualification tests are ongoing in support of the joint U.S./USSR SD flight demonstration project.[20]

Flux Tailoring

Verification of the optical alignment, solar simulator-to-concentrator-to-receiver optical interface surface was conducted in the thermal/vacuum environment of Tank 6 with the use of a rotating flux-distribution rake. The flux-distribution rake simulated the interior cylindrical surface of the solar receiver, which allows for direct measurement of the receiver flux. Comparison of the flux test data with analytical predictions showed excellent correlation. Further, the peak flux of 28.8 kW/m^2 compares to a worst-case prediction of 42.9 kW/m^2. Special test equipment was provided for facet alignment and flux distribution in Tank 6.[21]

Control Methodology

The SD system acceptance test included the concentrator, receiver, PCU, and WHR system in the Lewis thermal/vacuum facility with the advanced solar simulator. Acceptance testing of the SD system has successfully demonstrated startup, transient, and steady-state orbital operation and shutdown. About 2.0 kW (peak) (at 120 Vdc) of electrical power was achieved on Feb. 17, 1995 while operating at 52,000 rpm (design speed) with a turbine-inlet-temperature of 1063.5 K (1914.3°R) and a compressor-inlet-temperature (CIT) of 270.2 K (486.4°R). Illustrated in Fig. 7 is an example of steady-state orbital operation (over three orbits), while operating the TAC at 52,000 rpm. The average orbital user power produced was 1.83 kWe. About 107 We of the losses are from the power electronics contained in the PCCU. Additional accessory losses include the cooling pump and the shutdown valves that are estimated at 67 We. This simulated orbit provided 66 min of sunlight with 18 min of eclipse. Also shown is the average canister temperature and the receiver gas exit temperature.

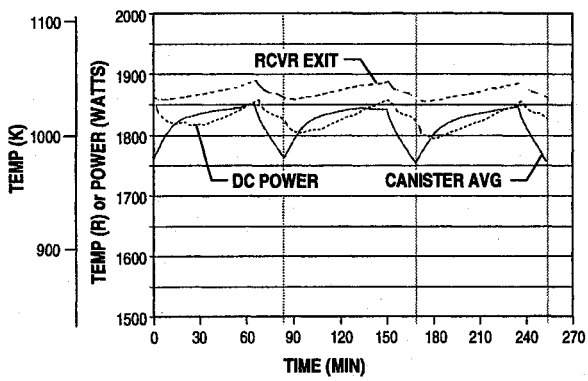

Fig. 7 Data showing steady-state orbital operation.

About 40 h of power operation with 10 orbits including five successful ambient starts with one hot restart were accumulated during acceptance testing. Ambient start temperature is defined as the receiver gas temperature at 294 K (530°R), whereas the hot start temperature is the receiver gas temperature above 778 K (1400°R). Early evaluation of performance data showed that steady-state and orbital operation of the PCU was as predicted.[22] Both thrust and journal bearing temperatures and rotor stability were shown to be within acceptable limits. During the acceptance testing the following conclusions were reached:

1) System starting was slower than analytical estimates because modeling ignored certain receiver mass elements that are not critical for analysis of orbital transients.

2) The receiver pressure drop was higher than anticipated because of the incorporation of heat transfer fins between the receiver tube and centerbody.

3) An overall system energy imbalance existed between receiver calorimetric calculations and solar simulator light measurements.

4) PCCU component problems associated with vacuum and cold environmental conditions were encountered.

Although differences were identified between the analytical models and the actual operation of individual components, the SD system has shown to be very reliable and robust. SD system testing performed by NASA has accumulated an additional 315 h of power operation including 177 simulated orbits (typically 66 min of sunlight/27 min of shade), and 11 ambient [294 K (530°R)] orbital starts, and 1 hot [778 K (1400°R)] restart.

Insolation Variations

Shown in Fig. 8 is a test that was conducted over a 40-h period with the TAC operating at 48,000 rpm and illustrates an orbital startup, steady-state orbital operation, and a shutdown. Data from the integrated SD system include the average

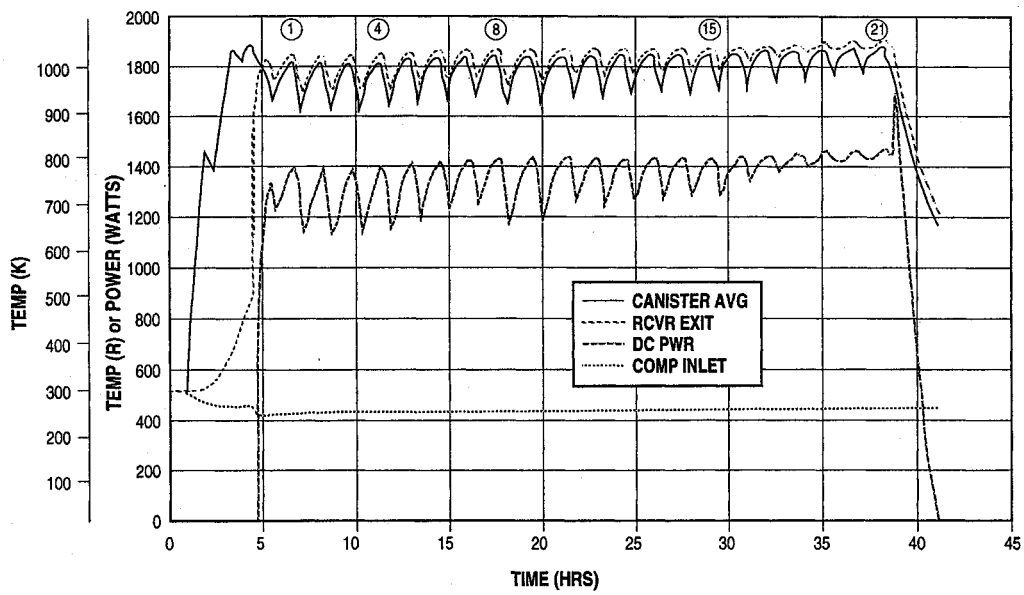

Fig. 8 Data showing startup, multiple orbits, and shutdown of the SD system.

receiver canister temperature, the receiver gas exit temperature, the CIT, and the dc power output as shown in Fig. 8. The solar simulator provided four different insolation levels: 1) 1.01, 2) 1.06, 3) 1.08, and 4) 1.14 suns (1.37 kW/m^2 = 1 sun), resulting in four steady-state orbital cases, during the 93-min orbit. The initial orbit that produces electrical power is identified as orbit 1. Balanced orbital operation was achieved on orbits 4, 8, 15, and 21. Balanced orbital operation is defined as repeatable conditions at the same time (sunrise or sunset) on successive orbits, <1.1 K (<2°R) change in receiver gas temperatures and <5 W change in power output. The first three cases (orbits 1–4, 5–8, and 9–15) are examples of operation of the heat receiver within the sensible heat regime (i.e., canister phase-change material not melted), which resulted in large temperature [137 K (2466°R)] and power (138 W) fluctuations. The fourth case (orbits 16–21) is in a latent heat receiver regime (i.e., phase-change material melted), which resulted in a marked reduction of temperature [19 K (34°R)] and power (49 W) fluctuations during the orbit. This is in good agreement with analytical predictions. The TAC was operating at 48,000 rpm during the test, except for the shutdown. Engine speed was increased to 52,000 rpm during the shutdown to speed up removal of the heat energy in the system. The 1.01 insolation case resulted in an overall system efficiency, sun into user energy, of 15%, with the engine efficiency of about 26%. Slight increases in both overall and engine efficiency were realized at the higher insolation levels.

An example of data from the orbital startup showing a representative solar receiver heating profile is shown in Fig. 9. The receiver canister temperature increases during each sun interval of the first three orbits until it reaches 1055 K (1900°R) during the third orbit. The turbine preheat requirement of 1055 K was established to overcome the potential of compressor surge effects that were observed during the hot-loop testing of the PCU. It was discovered during hot-loop testing that if the shutdown valves were left open and the TAC was motored, the turbine could be sufficiently preheated to eliminate surging of the compressor. Opening the shutdown valves that connect the compressor exit to the inlet was anticipated to eliminate the compressor surge problem because these work exactly like bleed valves used on open-cycle gas turbines for precisely the same purpose. Also shown are the receiver gas inlet and exit temperatures that gradually increased during the 3.5 h of heating.

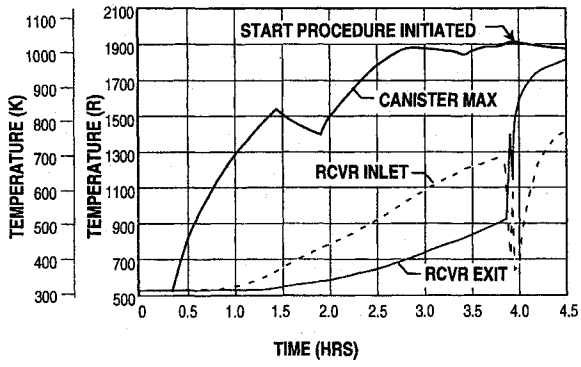

Fig. 9 Data showing ambient orbital startup.

After the canister reached 1055 K, the turbine preheat is conducted by motoring the TAC at 30,000 rpm, with the bypass (shutdown) valves open, for about 2 min. Note the relationship (reversal) of receiver inlet and exit temperatures during the 2-min preheat, indicating proper flow direction. Finally, with the bypass valves closed, the TAC is started by motoring at 36,000 rpm until self-sustained operation is observed. TAC motoring for this start required about 4 min.

Transient-Mode Performance

Figure 10 shows a test sequence that illustrates an orbital startup, steady-state and transient orbital operation, and a shutdown. Data from the SD system include the average receiver canister temperature, the receiver gas exit temperature, CIT, dc power output, and TAC speed, and are all shown in Fig. 10. This test was conducted over a 48-h period with the TAC operating at 44,000, 43,000, 52,000, and 54,000 rpm. The solar simulator provided approximately 1 sun (1.37 kW/m^2), with an orbit period of 66 min of sunlight and 27 min of shade, resulting in 27 simulated orbits producing power. Heating of the receiver cavity required three orbits to reach the startup criteria. The startup criteria is defined as the maximum receiver canister temperature greater than 1055 K (1900°R). The 1-sun insolation level corresponds to about 10 kW heat to the receiver. Balanced orbital operations were achieved on orbits 5 (@44,000 rpm), 14 (@43,000 rpm), 21 (@52,000 rpm), and 27 (@54,000 rpm). Table 1 summarizes the receiver and engine performance for the four balanced orbits. Average power output over the orbit ranged from 1.23 to 1.34 kW and engine efficiency (alternator output power divided by working fluid heat input) varied from 21.5 to 26.4%, whereas overall system efficiency ranged from 13.8 to 15%. Figure 11 shows the sen-

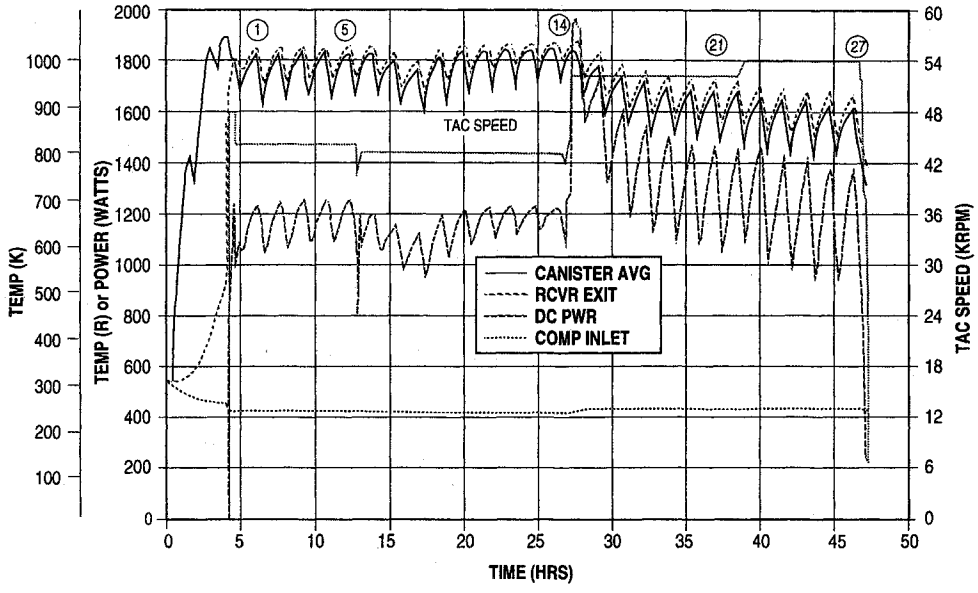

Fig. 10 Data show TAC speed changes (44, 43, 52, and 54 K rpm) for the PCU.

Table 1 SD system-balanced orbit performance data

Parameter	Orbit 5	14	21	27
Insolation, suns	0.99	1.02	1.00	0.98
ac power, kW	1.23	1.24	1.34	1.22
dc power, kW	1.18	1.19	1.28	1.17
Receiver exit, °R	1800	1842	1654	1595
Receiver inlet, °R	1542	1580	1384	1328
Compressor inlet, °R	425	420	434	435
TAC speed, rpm	44,163	43,143	52,127	54,016
Q_{GAS}, kW	4.69	4.67	5.62	5.70
Engine efficiency, %	26.2	26.4	23.9	21.5
Canister average, °R	1758	1802	1604	1543
Q_{LOSS}, kW	1.73	1.91	1.20	1.03
Q_{RCVR}, kW	9.06	9.27	9.61	9.48
Orbit efficiency, %	14.6	14.4	15.0	13.8

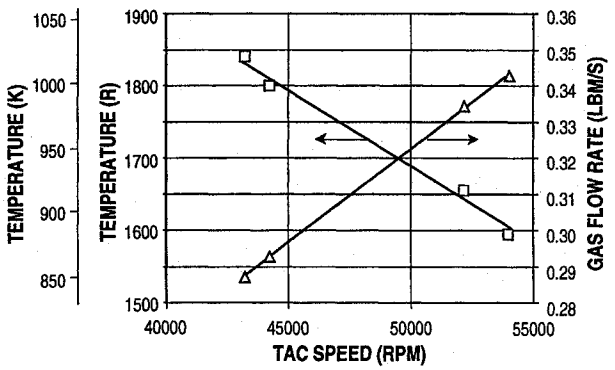

Fig. 11 Sensitivity of TAC speed to temperature and flow rate.

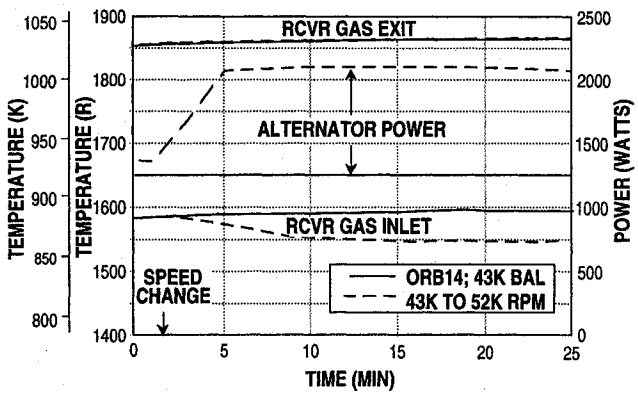

Fig. 12 Comparison of system response to TAC speed change (43–52 K rpm) vs balanced orbit (43 K rpm).

sitivity of the receiver gas exit temperature and gas flow rate to TAC speed. Orbit 14 provided the only example of operation in which the receiver was in the latent heat regime.

The sequence of the speed changes was selected to effect worst-case system performance transients. The change from 43,000 to 52,000 rpm, shown in Fig. 10, provides insight into the system response going from a hot, latent receiver to a sensible heat receiver. This speed change is similar to what could be expected on orbit in response to excessive receiver energy input (e.g., extended sun times caused by higher orbit inclinations). Figure 12 shows the short-term receiver gas temperature and power output effects of the speed change. The dashed lines represent the response to the speed transient and the solid lines provide a reference of the same parameters at the same time in the previous orbit. The data show essentially no change in receiver gas exit temperature and a minimal [about 27.8 K (50°R)] change in gas inlet temperature. As shown in Fig. 10, the long-term effect of the speed change was achieved six orbits (orbit 21) later upon achieving a balanced orbit at 52,000 rpm. The transition from balanced operation (orbit 14) at 43,000 rpm to balanced conditions at 52,000 rpm resulted in a sunset temperature (i.e., maximum orbital temperature) decrease at the receiver gas exit of 61 K (110°R). Similar results were obtained for the 52,000–54,000 rpm speed transient with minimal short-term effects and five transition orbits before the full impact of the speed change was observed on the receiver temperature.

Summary

Initial operational and performance data have demonstrated an SD power system that is of sufficient scale and fidelity to ensure confidence in the potential of SD technology for space. Integration of the solar concentrator and receiver has shown that peak fluxes within the receiver were well within worst-case design predictions. System testing has successfully shown orbital startup, transient and steady-state orbital operation, and shutdown in a relevant space environment with a simulated sun. Off-design thermodynamic performance data are provided that demonstrate the flexibility of the SD system under different solar intensities and operating speeds. Over 365 h of power operation, ranging from 400 W to 2.0 kWe of power operation, including 187 simulated orbits, 16 ambient starts, and 2 hot restarts have been completed.

SD system efficiencies during orbital operation have ranged from 13.8 to 16.1%. The demonstrated end-to-end system efficiency is very good when compared to large photovoltaic/battery systems. End-to-end orbital efficiencies of large photovoltaic/battery systems are currently estimated to be about 4% for the International Space Station. Testing to date has resulted in an improved understanding of integrated SD system operations and performance.

Acknowledgments

The collective efforts of the SD GTD Team have resulted in the world's first full-scale demonstration of a complete space-configured SD system in a large thermal/vacuum facility with a simulated sun. The authors acknowledge the contributions of the SD GTD Team members: NASA LeRC, Cleveland, Ohio, was responsible for overall project management and provided an advanced solar simulator with the large thermal/vacuum facility; Harris Corporation, Melbourne, Florida, for the offset solar concentrator; AlliedSignal Aerospace, Torrance, California, for the solar heat receiver (with thermal energy storage) and gas cooler; AlliedSignal Aerospace, Tempe, Arizona, for management of the industry team members and the power conversion system; Loral Vought Systems, Dallas, Texas, for the radiator panels; and Rockwell International Corporation, Rocketdyne Division, Canoga Park, California, for system integration and test support. Aerospace Design and Development (ADD), Niwot, Colorado, supplied the multilayer insulation for the heat receiver and power conversion subsystem; and Solar Kinetics Incorporated, Dallas, Texas, supplied the reflective facets for the concentrator.

References

[1]Shaltens, R. K., and Boyle, R. V., "Initial Results from the Solar Dynamic (SD) Ground Test Demonstration (GTD) Project at NASA Lewis," *Proceedings of the 30th Intersociety Energy Conversion Engineering Conference*, American Society of Mechanical Engineers, New York, 1995, pp. 363–368 (NASA TM 107004).

[2]Calogeras, J. E., and Dustin, M. O., "The Ground Testing of a 2kW$_e$ Solar Dynamic Space Power System," *Proceedings of the 27th Intersociety Energy Conversion Engineering Conference*, Vol. 1, Society of Automative Engineers, Warrendale, PA, 1992, pp. 455–460.

[3]Jefferies, K. S. (ed.), "Solar Dynamic Power System Development for Space Station *Freedom*," NASA RP1310, July 1993.

[4]Shaltens, R. K., "Overview of the Solar Dynamic Ground Test Demonstration Project at the NASA Lewis Research Center," NASA TM 106876, March 1995.

[5]Shaltens, R. K., and Boyle, R. V., "Update of the 2 kW Solar Dynamic Ground Test Demonstration Project," *Proceedings of the 29th Intersociety Energy Conversion Engineering Conference* (Monterey, CA), AIAA, Washington, DC, 1994, pp. 359–365 (NASA TM 105730).

[6]Shaltens, R. K., and Boyle, R. V., "Overview of the Solar Dynamic Ground Test Demonstration Project," *Proceedings of the 28th Intersociety Energy Conversion Engineering Conference*, American Chemical Society, Washington, DC, Vol. 2, 1993, pp. 831–836 (NASA TM 106296).

[7]Jefferies, K. S., "Solar Simulator for Solar Dynamic Space Power System Testing," *The 1994 ASME/JSME/JSES International Solar Energy Conference*, American Society of Mechanical Engineers, New York, 1994, pp. 217–222 (NASA TM 106393).

[8]Jaworske, D. A., Jefferies, K. S., and Mason, L. S., "Alignment and Initial Operation of an Advanced Solar Simulator," AIAA Paper 96-0102, Jan. 1996.

[9]Amundsen, P. C., and Harper, W. B., "BIPS Turboalternator-Compressor Characteristics and Application to the NASA Solar Dynamic Ground Demonstration Program," *Proceedings of the 27th Intersociety Energy Conversion Engineering Conference*, Vol. 2, Society of Automative Engingeers, Warrendale, PA, 1992, pp. 239–244.

[10]Schertz, P., Shabbar, S., and Lammert, L., "Development of an Improved Mirror Facet for Space Applications," NASA CR-189109, Oct. 1991.

[11]Bahnman, D. W., and Jensen, P. A., "Design of a Solar Concentrator for the Solar Dynamic Ground Test Demonstration Project," *The 1994 ASME/JSME/JSES International Solar Energy Conference* (San Francisco, CA), American Society of Mechanical Engineers, New York, 1994, pp. 193–203.

[12]Strumph, H. J., Westelaken, B., Shah, D., Pogue, B., Chin, Jr., Alvarez, J., and Klucher, B., "Fabrication and Testing of the Solar Dynamic Ground Test Demonstration Heat Receiver," *Proceedings of the 29th Intersociety Energy Conversion Engineering Conference* (Monterey, CA), AIAA, Washington, DC, 1994, pp. 372–377.

[13]De Groh, K. K., Roig, D. M., Burke, C. A., and Shah, D. R., "Performance and Durability of High Emittance Heat Receiver Surfaces for Solar Dynamic Power Systems," *The 1994 ASME/JSME/JSES International Solar Energy Conference* (San Francisco, CA), American Society of Mechanical Engineers, New York, 1994, pp. 251–264.

[14]Strumph, H. J., Avanessian, V., Ghafourian, R., and Huang, F. J., "Thermal and Structural Analysis of the Heat Receiver for the Solar Dynamic Ground Test Demonstrator," *The 1994 ASME/JSME/JSES International Solar Energy Conference* (San Francisco, CA), American Society of Mechanical Engineers, New York, 1994, pp. 223–234.

[15]Strumph, H. J., Krystkowiak, C., and Killackey, J. J., "Design of the Heat Receiver for the Solar Dynamic Ground Test Demonstrator Space Power System," *Proceedings of the 28th Intersociety Energy Conversion Engineering Conference*, American Chemical Society, Washington, DC, Vol. 1, 1993, pp. 469–475.

[16]Fleming, M. L., and Flores, R. R., "Radiator Selection for Space Station Solar Dynamic Power Systems," *Proceedings of the 22nd Intersociety Energy Conversion Engineering Conference*, AIAA, Washington, DC, 1987, pp. 208–213.

[17]Fleming, M. L., Flores, R. R., and Sharpe, R. R., "Solar Dynamic Ground Test Demonstration Radiator Design and Test," *Proceedings of the 29th Intersociety Energy Conversion Engineering Conference* (Monterey, CA), AIAA, Washington, DC, 1994, pp. 378–383.

[18]Fleming, M. L., and Flores, R. R., "Solar Dynamic Radiator Design Development," *The 1994 ASME/JSME/JSES International Solar Energy Conference* (San Francisco, CA), American Society of Mechanical Engineers, New York, 1994, pp. 245–250.

[19]Mason, L. S., and Kudija, C. J., "Solar Dynamic Ground Test Demonstration System Test Plans," *The 1994 ASME/JSME/JSES International Solar Energy Conference* (San Francisco, CA), American Society of Mechanical Engineers, New York, 1994, pp. 175–184.

[20]Huckins, E., and Ahlf, P., "Space Station Power Requirements and Issues," *Proceedings of the 29th Intersociety Energy Conversion Engineering Conference* (Monterey, CA), AIAA, Washington, DC, 1994, pp. 608–612.

[21]Campbell, J. S., and Jensen, P. A., "Design, Analysis and Test of a Solar Concentrator for Space Applications," *The 1994 ASME/JSME/JSES International Solar Energy Conference* (San Francisco, CA), American Society of Mechanical Engineers, New York, 1994, pp. 205–216.

[22]Mock, T. A., "Solar Dynamic Ground Test Demonstrator (SDGTD) System Orbital and Startup Control Methods," *The 1994 ASME/JSME/JSES International Solar Energy Conference* (San Francisco, CA), American Society of Mechanical Engineers, New York, 1994, pp. 185–191.